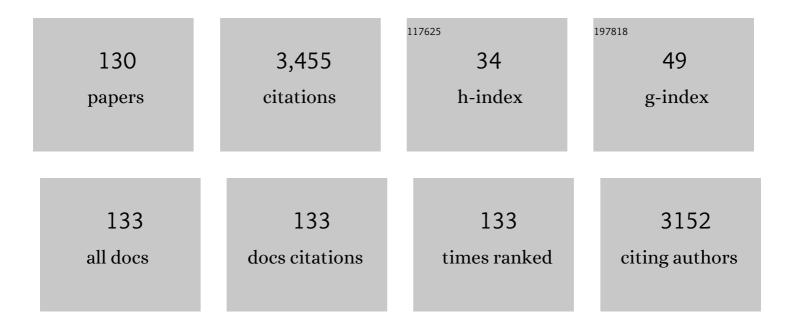
List of Publications by Year in descending order

Source: https://exaly.com/author-pdf/149176/publications.pdf Version: 2024-02-01



Томсти

#	Article	IF	CITATIONS
1	Experimental study on the petrophysical variation of different rank coals with microwave treatment. International Journal of Coal Geology, 2016, 154-155, 82-91.	5.0	104
2	Dysregulated N6â€methyladenosineÂmethylation writer METTL3 contributes to the proliferation and migration of gastric cancer. Journal of Cellular Physiology, 2020, 235, 548-562.	4.1	96
3	High temperature solid oxide H2O/CO2 co-electrolysis for syngas production. Fuel Processing Technology, 2017, 161, 248-258.	7.2	95
4	Comprehensive analysis of prognostic immuneâ€related genes in the tumor microenvironment of cutaneous melanoma. Journal of Cellular Physiology, 2020, 235, 1025-1035.	4.1	95
5	Syngas production on a symmetrical solid oxide H2O/CO2 co-electrolysis cell with Sr2Fe1.5Mo0.5O6–Sm0.2Ce0.8O1.9 electrodes. Journal of Power Sources, 2016, 305, 240-248.	7.8	90
6	Dynamic diffusion-based multifield coupling model for gas drainage. Journal of Natural Gas Science and Engineering, 2017, 44, 233-249.	4.4	86
7	Sr ₂ Fe _{1.5} Mo _{0.5} O _{6â^î^} - Sm _{0.2} Ce _{0.8} O _{1.9} Composite Anodes for Intermediate-Temperature Solid Oxide Fuel Cells. Journal of the Electrochemical Society, 2012, 159, B619-B626.	2.9	73
8	In-situ exsolution of nanoparticles from Ni substituted Sr2Fe1.5Mo0.5O6 perovskite oxides with different Ni doping contents. Electrochimica Acta, 2020, 348, 136351.	5.2	73
9	Thermodynamic analysis and optimization of photovoltaic/thermal hybrid hydrogen generation system based on complementary combination of photovoltaic cells and proton exchange membrane electrolyzer. Energy Conversion and Management, 2019, 183, 97-108.	9.2	71
10	In vitro evaluation of nanoplastics using human lung epithelial cells, microarray analysis and co-culture model. Ecotoxicology and Environmental Safety, 2021, 226, 112837.	6.0	70
11	Immune cell infiltration as a biomarker for the diagnosis and prognosis of digestive system cancer. Cancer Science, 2019, 110, 3639-3649.	3.9	67
12	Development of tungsten stabilized SrFe0.8W0.2O3-δ material as novel symmetrical electrode for solid oxide fuel cells. Journal of Power Sources, 2020, 455, 227951.	7.8	66
13	Coal Permeability Evolution and Gas Migration Under Non-equilibrium State. Transport in Porous Media, 2017, 118, 393-416.	2.6	63
14	Zr0.84Y0.16O1.92–La0.8Sr0.2Cr0.5Fe0.5O3â^î^́ dual-phase composite hollow fiber membrane targeting chemical reactor applications. Journal of Membrane Science, 2012, 389, 435-440.	8.2	62
15	Steam electrolysis in a solid oxide electrolysis cell fabricated by the phase-inversion tape casting method. Electrochemistry Communications, 2015, 61, 106-109.	4.7	62
16	A robust solid oxide electrolyzer for highly efficient electrochemical reforming of methane and steam. Journal of Materials Chemistry A, 2019, 7, 13550-13558.	10.3	58
17	A Novel Cobalt-Free, CO ₂ -Stable, and Reduction-Tolerant Dual-Phase Oxygen-Permeable Membrane. ACS Applied Materials & Interfaces, 2013, 5, 11038-11043.	8.0	53
18	Fabrication and catalytic growth mechanism of mullite ceramic whiskers using molybdenum oxide as catalyst. Ceramics International, 2017, 43, 2871-2875.	4.8	51

#	Article	IF	CITATIONS
19	Improvement of output performance of solid oxide fuel cell by optimizing the active anode functional layer. Electrochimica Acta, 2019, 298, 112-120.	5.2	51
20	Improving the chemical stability of BaCe0.8Sm0.2O3â^'δ electrolyte by Cl doping for proton-conducting solid oxide fuel cell. Electrochemistry Communications, 2013, 28, 87-90.	4.7	50
21	p21-activated Kinase 6 (PAK6) Inhibits Prostate Cancer Growth via Phosphorylation of Androgen Receptor and Tumorigenic E3 Ligase Murine Double Minute-2 (Mdm2). Journal of Biological Chemistry, 2013, 288, 3359-3369.	3.4	50
22	A novel clean and effective syngas production system based on partial oxidation of methane assisted solid oxide co-electrolysis process. Journal of Power Sources, 2015, 277, 261-267.	7.8	50
23	Thermal Stability of an in Situ Exsolved Metallic Nanoparticle Structured Perovskite Type Hydrogen Electrode for Solid Oxide Cells. ACS Sustainable Chemistry and Engineering, 2019, 7, 17834-17844.	6.7	50
24	Molecular cloning and sequence analysis of heat shock proteins 70 (HSP70) and 90 (HSP90) and their expression analysis when exposed to benzo(a)pyrene in the clam Ruditapes philippinarum. Gene, 2015, 555, 108-118.	2.2	49
25	Robust redox-reversible perovskite type steam electrolyser electrode decorated with <i>in situ</i> exsolved metallic nanoparticles. Journal of Materials Chemistry A, 2020, 8, 582-591.	10.3	47
26	Microstructure Tailoring of the Nickel Oxide–Yttria-Stabilized Zirconia Hollow Fibers toward High-Performance Microtubular Solid Oxide Fuel Cells. ACS Applied Materials & Interfaces, 2014, 6, 18853-18860.	8.0	46
27	In-situ growth of metallic nanoparticles on perovskite parent as a hydrogen electrode for solid oxide cells. Journal of Power Sources, 2018, 405, 114-123.	7.8	45
28	The co-electrolysis of CO ₂ –H ₂ O to methane via a novel micro-tubular electrochemical reactor. Journal of Materials Chemistry A, 2017, 5, 2904-2910.	10.3	43
29	Supramolecular Chirality from Hierarchical Self-Assembly of Atomically Precise Silver Nanoclusters Induced by Secondary Metal Coordination. ACS Nano, 2021, 15, 15910-15919.	14.6	42
30	Fabrication of micro-tubular solid oxide fuel cells using sulfur-free polymer binder via a phase inversion method. Journal of Power Sources, 2015, 290, 1-7.	7.8	40
31	PAK1-mediated MORC2 phosphorylation promotes gastric tumorigenesis. Oncotarget, 2015, 6, 9877-9886.	1.8	39
32	Multiscale porous Fe–N–C networks as highly efficient catalysts for the oxygen reduction reaction. Nanoscale, 2019, 11, 19506-19511.	5.6	38
33	Efficient syngas generation for electricity storage through carbon gasification assisted solid oxide co-electrolysis. Applied Energy, 2016, 173, 52-58.	10.1	36
34	A Thermoelectric Power Sensor and Its Package Based on MEMS Technology. Journal of Microelectromechanical Systems, 2012, 21, 121-131.	2.5	35
35	Systematic analyses of a novel IncRNA-associated signature as the prognostic biomarker for Hepatocellular Carcinoma. Cancer Medicine, 2018, 7, 3240-3256.	2.8	35
36	Optimization of Indirectly-Heated Type Microwave Power Sensors Based on GaAs Micromachining. IEEE Sensors Journal, 2012, 12, 1349-1355.	4.7	34

#	Article	IF	CITATIONS
37	Molecular characterization of lung adenocarcinoma: A potential four–long noncoding RNA prognostic signature. Journal of Cellular Biochemistry, 2019, 120, 705-714.	2.6	33
38	An integrated technology for gas control and green mining in deep mines based on ultra-thin seam mining. Environmental Earth Sciences, 2017, 76, 1.	2.7	32
39	Assessing the moisture migration during microwave drying of coal using low-field nuclear magnetic resonance. Drying Technology, 2018, 36, 567-577.	3.1	31
40	Enhanced water desalination performance through hierarchically-structured ceramic membranes. Journal of the European Ceramic Society, 2017, 37, 2431-2438.	5.7	30
41	Ni infiltrated Sr2Fe1.5Mo0.5O6-δ-Ce0.8Sm0.2O1.9 electrode for methane assisted steam electrolysis process. Electrochemistry Communications, 2017, 79, 63-67.	4.7	30
42	Enhancing the Oxygen Permeation Rate of Zr _{0.84} Y _{0.16} O _{1.92} –La _{0.8} Sr _{0.2} Cr _{0.5Dual-Phase Hollow Fiber Membrane by Coating with Ce_{0.8}Sm_{0.2}O_{1.9} Nanoparticles. ACS Applied Materials & amp;}	ub>Fe <su 8.0</su 	b>0.5 29
43	Interfaces, 2013, 5, 9454-9460. Novel light-weight, high-performance anode-supported microtubular solid oxide fuel cells with an active anode functional layer. Journal of Power Sources, 2015, 293, 852-858.	7.8	29
44	The beneficial effects of straight open large pores in the support on steam electrolysis performance of electrode-supported solid oxide electrolysis cell. Journal of Power Sources, 2018, 374, 175-180.	7.8	29
45	Deep sequencing-based transcriptome profiling analysis of Chlamys farreri exposed to benzo[a]pyrene. Gene, 2014, 551, 261-270.	2.2	28
46	Deep sequencing of the scallop Chlamys farreri transcriptome response to tetrabromobisphenol A (TBBPA) stress. Marine Genomics, 2015, 19, 31-38.	1.1	28
47	Environmental toxicology wars: Organ-on-a-chip for assessing the toxicity of environmental pollutants. Environmental Pollution, 2021, 268, 115861.	7.5	28
48	A dual-phase bilayer oxygen permeable membrane with hierarchically porous structure fabricated by freeze-drying tape-casting method. Journal of Membrane Science, 2016, 520, 354-363.	8.2	27
49	Trends on PM2.5 research, 1997–2016: a bibliometric study. Environmental Science and Pollution Research, 2018, 25, 12284-12298.	5.3	27
50	Understanding the A-site non-stoichiometry in perovskites: promotion of exsolution of metallic nanoparticles and the hydrogen oxidation reaction in solid oxide fuel cells. Sustainable Energy and Fuels, 2021, 5, 401-411.	4.9	26
51	Methane assisted solid oxide co-electrolysis process for syngas production. Journal of Power Sources, 2017, 344, 119-127.	7.8	25
52	Solvent effects on the morphology and performance of the anode substrates for solid oxide fuel cells. Journal of Power Sources, 2017, 363, 304-310.	7.8	25
53	The Combination of a Biocontrol Agent TrichodermaÂasperellum SC012 and Hymexazol Reduces the Effective Fungicide Dose to Control Fusarium Wilt in Cowpea. Journal of Fungi (Basel, Switzerland), 2021, 7, 685.	3.5	25
54	A cobalt-free composite cathode prepared by a superior method for intermediate temperature solid oxide fuel cells. Journal of Power Sources, 2012, 217, 431-436.	7.8	23

#	Article	IF	CITATIONS
55	Effect of casting slurry composition on anode support microstructure and cell performance of MT-SOFCs by phase inversion method. Electrochimica Acta, 2014, 149, 159-166.	5.2	23
56	A straight, open and macro-porous fuel electrode-supported protonic ceramic electrochemical cell. Journal of Materials Chemistry A, 2021, 9, 10789-10795.	10.3	23
57	Enhancing performance of molybdenum doped strontium ferrite electrode by surface modification through Ni infiltration. International Journal of Hydrogen Energy, 2021, 46, 10876-10891.	7.1	23
58	Performance and distribution of relaxation times analysis of Ruddlesden-Popper oxide Sr3Fe1.3Co0.2Mo0.5O7-l´as a potential cathode for protonic solid oxide fuel cells. Electrochimica Acta, 2020, 352, 136444.	5.2	23
59	Ce _{0.8} Sm _{0.2} O _{1.9} –La _{0.8} Sr _{0.2} Cr _{0.5Dual-Phase Hollow Fiber Membranes Operated under Different Gradients. Industrial & Engineering Chemistry Research, 2014, 53, 6131-6136.}	b>Fe _{ 3.7}	>0.5€ 22
60	High photocatalytic property and crystal growth of spindle-like ZnO microparticles synthesized by one-step hydrothermal method. Vacuum, 2017, 144, 229-236.	3.5	22
61	Preparation and characterization of a redox-stable Pr0.4Sr0.6Fe0.875Mo0.125O3-δ material as a novel symmetrical electrode for solid oxide cell application. International Journal of Hydrogen Energy, 2020, 45, 21825-21835.	7.1	22
62	Tailoring the pore structure of cathode supports for improving the electrochemical performance of solid oxide fuel cells. Journal of Electroceramics, 2018, 40, 138-143.	2.0	21
63	Integrated analysis of two-lncRNA signature as a potential prognostic biomarker in cervical cancer: a study based on public database. PeerJ, 2019, 7, e6761.	2.0	21
64	Effect of PEG additive on anode microstructure and cell performance of anode-supported MT-SOFCs fabricated by phase inversion method. Journal of Power Sources, 2015, 279, 774-780.	7.8	20
65	RNA-seq based on transcriptome reveals differ genetic expressing in Chlamys farreri exposed to carcinogen PAHs. Environmental Toxicology and Pharmacology, 2015, 39, 313-320.	4.0	20
66	A Highly-Performed, Dual-Layered Cathode Supported Solid Oxide Electrolysis Cell for Efficient CO ₂ Electrolysis Fabricated by Phase Inversion Co-Tape Casting Method. Journal of the Electrochemical Society, 2017, 164, F1130-F1135.	2.9	20
67	<p>TheÂN6-Methyladenosine (m6A) Methylation GeneÂYTHDF1ÂReveals aÂPotential Diagnostic Role for Gastric Cancer</p> . Cancer Management and Research, 2020, Volume 12, 11953-11964.	1.9	20
68	Bioaccumulation and oxidative damage of polycyclic aromatic hydrocarbon mixtures in Manila clam Ruditapes philippinarum. Ecotoxicology and Environmental Safety, 2020, 197, 110558.	6.0	20
69	Nanomaterials-induced toxicity on cardiac myocytes and tissues, and emerging toxicity assessment techniques. Science of the Total Environment, 2021, 800, 149584.	8.0	18
70	Robust Ruddlesdenâ€Popper phase Sr ₃ Fe _{1.3} Mo _{0.5} N _{i0.2} O _{7â€Î´} decorated with inâ€situ exsolved Ni nanoparticles as an efficient anode for hydrocarbon fueled solid oxide fuel cells. SusMat, 2022, 2, 487-501.	14.9	18
71	Modeling of hydrogen permeation for Ni–ceramic proton conductor composite membrane with symmetric structure. Journal of Membrane Science, 2012, 415-416, 328-335.	8.2	16
72	Preparation and oxygen permeability of Ce0.8Sm0.2O2â^ʾδ-La0.7Ca0.3CrO3â^ʾδ dual-phase composite hollow fiber membrane. Solid State Ionics, 2012, 225, 690-694.	2.7	16

#	Article	IF	CITATIONS
73	Molecular characterization of papillary thyroid carcinoma: a potential three-lncRNA prognostic signature. Cancer Management and Research, 2018, Volume 10, 4297-4310.	1.9	16
74	Solid oxide fuel cells supported on cathodes with large straight open pores and catalyst-decorated surfaces. Solid State Ionics, 2018, 323, 130-135.	2.7	16
75	Rapid and mass production of biopesticide Trichoderma Brev T069 from cassava peels using newly established solid-state fermentation bioreactor system. Journal of Environmental Management, 2022, 313, 114981.	7.8	16
76	Differential gene expression analysis of benzo(a)pyrene toxicity in the clam, Ruditapes philippinarum. Ecotoxicology and Environmental Safety, 2015, 115, 126-136.	6.0	15
77	Expression of miRâ€486â€5p and its signiï¬cance in lung squamous cell carcinoma. Journal of Cellular Biochemistry, 2019, 120, 13912-13923.	2.6	15
78	Prognostic value of a twoâ€microRNA signature for papillary thyroid cancer and a bioinformatic analysis of their possible functions. Journal of Cellular Biochemistry, 2019, 120, 7185-7198.	2.6	15
79	Global sensitivity analysis of solid oxide fuel cells with Bayesian sparse polynomial chaos expansions. Applied Energy, 2020, 260, 114318.	10.1	15
80	Co-generation of liquid chemicals and electricity over Co-Fe alloy/perovskite anode catalyst in a propane fueled solid oxide fuel cell. Separation and Purification Technology, 2022, 291, 120890.	7.9	15
81	The two-fold diffusion process for proton uptake reaction in BCFZY e-/H+/O2- triple conductor measured by electrical conductivity relaxation. Ionics, 2020, 26, 5293-5297.	2.4	14
82	Experimental Research on Water Migration-Damage Characteristics of Lignite under Microwave Heating. Energy & Fuels, 2021, 35, 1058-1069.	5.1	14
83	Comprehensive analysis of a novel IncRNA profile reveals potential prognostic biomarkers in clear cell renal cell carcinoma. Oncology Reports, 2018, 40, 1503-1514.	2.6	13
84	Robust Freeze-Cast Bilayer Dual-Phase Oxygen Transport Membrane Targeting Chemical Reactor Application. ACS Applied Nano Materials, 2018, 1, 3774-3778.	5.0	13
85	Oxygen permeability and CO2-tolerance of Sr(Co0.8Fe0.2)0.8Ti0.2O3â^î^Î^hollow fiber membrane. Separation and Purification Technology, 2011, 77, 76-79.	7.9	12
86	Zr0.84Y0.16O1.92 –La0.8Sr0.2Cr0.5Fe0.5O3â^'δ composite membrane for CO2 decomposition. Materials Letters, 2012, 86, 5-8.	2.6	12
87	Determination of Phase Volume Fractions of Ceramic Composite by Synchrotron Radiation Computed Tomography. Journal of the American Ceramic Society, 2012, 95, 2667-2671.	3.8	12
88	Fabrication and Properties of Electrospun and Electrosprayed Polyethylene Glycol/Polylactic Acid (PEG/PLA) Films. Coatings, 2021, 11, 790.	2.6	12
89	A novel salt-tolerant strain Trichoderma atroviride HN082102.1 isolated from marine habitat alleviates salt stress and diminishes cucumber root rot caused by Fusarium oxysporum. BMC Microbiology, 2022, 22, 67.	3.3	12
90	Upregulated LMO1 in prostate cancer acts as a novel coactivator of the androgen receptor. International Journal of Oncology, 2015, 47, 2181-2187.	3.3	11

#	Article	IF	CITATIONS
91	A novel <i>Trichoderma asperellum</i> strain DQ-1 promotes tomato growth and induces resistance to gray mold caused by <i>Botrytis cinerea</i> . FEMS Microbiology Letters, 2021, 368, .	1.8	11
92	Engineering the wetting behavior of ceramic membrane by carbon nanotubes via a chemical vapor deposition technique. Journal of Membrane Science, 2022, 648, 120357.	8.2	11
93	Study of Effects of Hard Thick Roof on Gas Migration and Field Experiment of Roof Artificially Guided Pre-splitting for Efficient Gas Control. Natural Resources Research, 2020, 29, 1819-1841.	4.7	10
94	A safe mining approach for deep outburst coal seam groups with hardâ€ŧhick sandstone roof: Stepwise risk control based on gas diversion and extraction. Energy Science and Engineering, 2020, 8, 2946-2965.	4.0	10
95	Performance and mechanism of a novel woodchip embedded biofilm electrochemical reactor (WBER) for nitrate-contaminated wastewater treatment. Chemosphere, 2021, 276, 130250.	8.2	10
96	Molecular characterization of lung cancer: A twoâ€miRNA prognostic signature based on cancer stemâ€like cells related genes. Journal of Cellular Biochemistry, 2020, 121, 2889-2900.	2.6	9
97	The benefits of smoking cessation on survival in cancer patients by integrative analysis of multiâ€omics data. Molecular Oncology, 2020, 14, 2069-2080.	4.6	9
98	Simultaneous water and electricity harvesting from low-grade heat by coupling a membrane distiller and an electrokinetic power generator. Journal of Materials Chemistry A, 2021, 9, 27709-27717.	10.3	9
99	Source risk, ecological risk, and bioeffect assessment for polycyclic aromatic hydrocarbons (PAHs) in Laizhou Bay and Jiaozhou Bay of Shandong Peninsula, China. Environmental Science and Pollution Research, 2022, 29, 56705-56726.	5.3	9
100	Identification of interacting proteins with aryl hydrocarbon receptor in scallop Chlamys farreri by yeast two hybrid screening. Ecotoxicology and Environmental Safety, 2016, 133, 381-389.	6.0	7
101	Catalytic effect of (Ti _{0.85} Zr _{0.15}) _{1.05} Mn _{1.2} Cr _{0.6} V _{0.1hydrogen storage properties of ultrafine magnesium particles. RSC Advances, 2017, 7, 34538-34547.}	b> &ø <sut< td=""><td>o>071⊂</td></sut<>	o>071⊂
102	Anaerobic Bioremediation Performance and Indigenous Microbial Communities in Treatment of Trichloroethylene/Nitrate-Contaminated Groundwater. Environmental Engineering Science, 2018, 35, 311-322.	1.6	7
103	Automated Vulnerability Discovery and Exploitation in the Internet of Things. Sensors, 2019, 19, 3362.	3.8	7
104	Pr and Mo Coâ€Đoped SrFeO _{3–<i>δ</i>} as an Efficient Cathode for Pure CO ₂ Reduction Reaction in a Solid Oxide Electrolysis Cell. Energy Technology, 2020, 8, 2000539.	3.8	7
105	Titanium dioxide nanoparticles induced the apoptosis of RAW264.7 macrophages through miR-29b-3p/NFAT5 pathway. Environmental Science and Pollution Research, 2020, 27, 26153-26162.	5.3	7
106	Growing and Pruning Selective Ensemble Regression for Nonlinear and Nonstationary Systems. IEEE Access, 2020, 8, 73278-73292.	4.2	7
107	N6-methyladenosine RNA modification and its interaction with regulatory non-coding RNAs in colorectal cancer. RNA Biology, 2021, 18, 551-561.	3.1	7
108	Robust <i>in situ</i> exsolved nanocatalysts on perovskite oxide as an efficient anode for hydrocarbon fueled solid oxide fuel cells. Sustainable Energy and Fuels, 2022, 6, 1373-1381.	4.9	7

#	Article	IF	CITATIONS
109	Excessive alcohol consumption and the risk of knee osteoarthritis: a prospective study from the Osteoarthritis Initiative. Osteoarthritis and Cartilage, 2022, 30, 697-701.	1.3	7
110	Chaotic Time-Delay Signature Suppression and Entropy Growth Enhancement Using Frequency-Band Extractor. Entropy, 2021, 23, 516.	2.2	6
111	Dietary patterns and risk of developing knee osteoarthritis: data from the osteoarthritis initiative. Osteoarthritis and Cartilage, 2021, 29, 834-840.	1.3	6
112	A highly active and stable Sr2Fe1.5Mo0.5O6-δ-Ce0.8Sm0.2O1.95 ceramic fuel electrode for efficient hydrogen production via a steam electrolyzer without safe gas. International Journal of Coal Science and Technology, 2022, 9, 1.	6.0	6
113	Advanced Ruâ€Infiltrated Perovskite Oxide Electrodes for Boosting the Performance of Syngas Fueled Solid Oxide Fuel Cell. ChemElectroChem, 2022, 9, .	3.4	6
114	High frequency properties of Fe73.5Cu1Nb3Si13.5B9/Zn0.5Ni0.5Fe2O4 soft magnetic composite with micro-cellular structure. Science China: Physics, Mechanics and Astronomy, 2012, 55, 2392-2396.	5.1	5
115	Modeling of hydrogen permeation for Ni–BZCY asymmetric membrane. Journal of Membrane Science, 2013, 437, 196-204.	8.2	5
116	Fabrication of high toughness alumina with elongated grains. Journal of Materials Science Letters, 2001, 20, 1425-1427.	0.5	4
117	Identification of microRNA-like RNAs from Trichoderma asperellum DQ-1 during its interaction with tomato roots using bioinformatic analysis and high-throughput sequencing. PLoS ONE, 2021, 16, e0254808.	2.5	3
118	Emerging Roles of N6-Methyladenosine Demethylases and Its Interaction with Environmental Toxicants in Digestive System Cancers. Cancer Management and Research, 2021, Volume 13, 7101-7114.	1.9	3
119	Conversion of Dagang Vacuum Residue into Oxygen-Containing Organic Compounds by Photo-Oxidation withH2O2overTiO2. International Journal of Photoenergy, 2011, 2011, 1-9.	2.5	2
120	A stability condition of zero dynamics of a discrete time systems with backward triangle sample and hold. , 2017, , .		2
121	Precise Photon Correlation Measurement of a Chaotic Laser. Applied Sciences (Switzerland), 2019, 9, 4907.	2.5	2
122	Expert Control System based Hierarchical Control Strategy for Tunnel Microwave Rice Drying. , 2019, ,		2
123	High-Quality Genome Sequence Data of <i>Trichoderma gracile</i> HK011-1, a Fungal Antagonistic Agent Against Plant Pathogens. Plant Disease, 2022, 106, 1035-1038.	1.4	2
124	Real-time and visual detection of Cercospora canescens based on the cytb gene using loop-mediated isothermal amplification (LAMP). Canadian Journal of Plant Pathology, 2021, 43, 551-558.	1.4	1
125	Structural Characteristics and Properties of Polylactic Acid (PLA) and Cellulose Triacetate (CTA) Fibers for Heat-Not-Burn (HNB) Cigarettes. IOP Conference Series: Earth and Environmental Science, 2021, 719, 042044.	0.3	1
126	The Highly Contiguous Genome Resource of <i>Trichoderma semiorbis</i> FJ059, a Biological Control Agent for Litchi Downy Blight. Phytopathology, 2022, 112, 1391-1395.	2.2	1

#	Article	IF	CITATIONS
127	Nanoporous Polymer Films from Immiscible Polymer Blends: Pore Size and Composition Dependence. Materials Research Society Symposia Proceedings, 2004, 856, BB10.13.1.	0.1	Ο
128	High Performance Solid Oxide Electrolysis Cells with Hierarchically Porous Ni-YSZ Electrode. ECS Transactions, 2017, 78, 3217-3228.	0.5	0
129	A Real- Time Vessel- Buoy Collision Risk Estimation Model for Inland Waterway Navigation. , 2018, , .		Ο
130	AutoDE: Automated Vulnerability Discovery and Exploitation. , 2019, , .		0